

The Coupling Impedance of the RHIC Injection Kicker System

H. Hahn

August 1996

Collider Accelerator Department
Brookhaven National Laboratory

U.S. Department of Energy

USDOE Office of Science (SC)

Notice: This technical note has been authored by employees of Brookhaven Science Associates, LLC under Contract No. DE-AC02-76CH00016 with the U.S. Department of Energy. The publisher by accepting the technical note for publication acknowledges that the United States Government retains a non-exclusive, paid-up, irrevocable, world-wide license to publish or reproduce the published form of this technical note, or allow others to do so, for United States Government purposes.

DISCLAIMER

This report was prepared as an account of work sponsored by an agency of the United States Government. Neither the United States Government nor any agency thereof, nor any of their employees, nor any of their contractors, subcontractors, or their employees, makes any warranty, express or implied, or assumes any legal liability or responsibility for the accuracy, completeness, or any third party's use or the results of such use of any information, apparatus, product, or process disclosed, or represents that its use would not infringe privately owned rights. Reference herein to any specific commercial product, process, or service by trade name, trademark, manufacturer, or otherwise, does not necessarily constitute or imply its endorsement, recommendation, or favoring by the United States Government or any agency thereof or its contractors or subcontractors. The views and opinions of authors expressed herein do not necessarily state or reflect those of the United States Government or any agency thereof.

RHIC PROJECT
Brookhaven National Laboratory

**The Coupling Impedance of the
RHIC Injection Kicker System**

H. Hahn and A. Ratti

August 1996

H. Hahn and A. Ratti

The RHIC injection kicker is configured as a "C" cross section magnet with interspersed ferrite¹ (Nickel-Zinc ferrite with high permeability and resistivity for use at frequencies up to ~100 MHz) and dielectric² (sintered mixture of Magnesium Titanat and Calcium Titanat with high dielectric constant $\epsilon \sim 100$) blocks as shown in Fig. 1. The deflection properties of the kicker are dominated (~85%) by the magnetic field and thus by the ferrite properties and its geometrical configuration. The dielectric blocks provide the capacitance required to achieve a transmission line kicker (<50 nsec current rise time) and to reduce the characteristic impedance so as to match the $50/2 \Omega$ of the Blumlein pulser. The dielectric blocks impose the de-facto voltage limit of the kicker and represent one of the primary design limitations.



²MCT-100 by Trans-Tech, Inc., Adamstown, Maryland.

The longitudinal coupling impedance of a half-size kicker model was previously measured by Mane et al³ with the results raising some concern due to the presence of sharp resonances in the GHz region. A more extensive study identified the origin of these resonances as local resonances in the dielectric blocks exposed to the beam.⁴ In the present kicker configuration, the so-called "hybrid" version, the resonances were completely suppressed by removing the dielectric blocks at the sides and replacing them by ferrite.

In this report, measured results for the longitudinal coupling impedance of a half-size "hybrid" injection kicker, both free-standing as well as part of the kicker system with Blumlein pulser, are presented. A schematic of the kicker system is shown in Fig. 2. The coupling impedance was measured by the established wire method which however, in order to yield accurate results, had to be interpreted via the log-formula for a distributed impedance.

In summary, the total coupling impedance contribution of four full-size RHIC injection kickers with their ceramic beam tube is $Z/n \leq 0.22 \Omega/\text{ring}$ in the frequency range from 0.1 to 1 GHz, and less at higher frequencies. It is to be noted, that the coupling impedance above 100 MHz is completely ferrite dominated and is decoupled from the pulser system. At lower frequencies, the pulser with the ~ 75 m long cables between pulser and kicker make a small contribution. Overall, one finds that the kicker coupling impedance is tolerable without the need for special impedance-reduction measures.

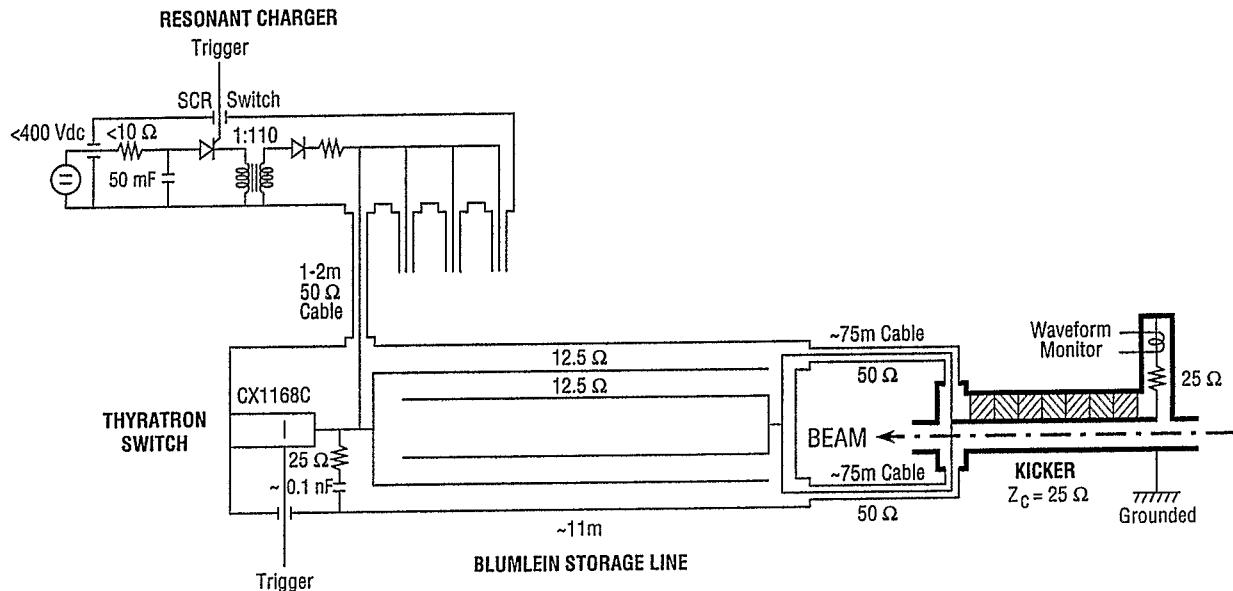


Fig. 2. Kicker System.

³V. Mane, S. Peggs, D. Trbojevic, W. Zhang, Proc. 1995 PAC, Dallas, TX, p. 3134.

⁴H. Hahn, M. Morvillo, A. Ratti, BNL Report AD/RHIC/RD-95 (1995).

II. WIRE MEASUREMENT OF THE COUPLING IMPEDANCE

The coupling impedance was measured using the wire method in which a resistive match provides a smooth transition from the 50 Ω of the network analyzer to the characteristic impedance of the reference line in the setup.⁵ The advantage of this method stems from the simplicity of its calibration procedure and the fact that a sufficient approximation of the results for the impedance in terms of real/imaginary or amplitude/phase is directly provided by the network analyzer and can be plotted without post processing. However the results quoted above were obtained using the more accurate "log-formula" appropriate for distributed systems.

The coupling impedance of the kicker system was measured with the existing bench setup for wire measurements previously used and described,⁴ with its schematic shown in Fig. 3. The measurements were performed with the Hewlett-Packard Network Analyzer 8753C connected to the S-Parameter Test Set 85078A.

The characteristic impedance of the connecting reference waveguides was measured directly to be $Z_{ref} = 165 \Omega$ by shorting the output port of a waveguide section, for which the input impedance becomes

$$Z_{in} = Z_{ref} \tan \left(\frac{\pi f}{2 f_{\lambda/4}} \right)$$

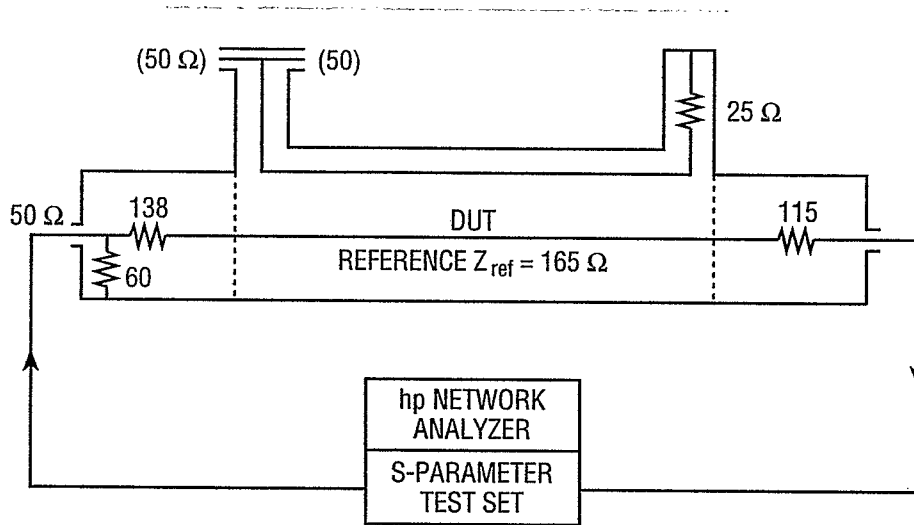


Fig. 3. Wire measurement of coupling impedance.

⁵A. Ratti, Fourth EPAC, London 1994, vol. 2, p. 1262.

The wire measurement of the coupling impedance is simplified, calibration errors are reduced, and post-processing of data is avoided by matching the 50 Ω of the network analyzer to the 165 Ω of the reference line. Here a solution with a resistive match was used. At the input port, a parallel resistor of $\sim 59.9 \Omega$ and a series resistor of 137.7 Ω provides forward and backward matching. At the output port, a series resistor of $\sim 115 \Omega$ provides forward matching. The frequency dependence of the carbon resistors and stray inductances/capacitances destroys the match at higher frequencies, but is corrected by the calibration procedure.

The coupling impedance measurement is obtained from the change in the forward scattering coefficient S_{21DUT} with respect to the reference measuring system with S_{21ref} (which by proper calibration can be made to be $S_{21ref} = 1$). In the case of a single lumped disturbance, and as a first approximation in the case of a distributed impedance (such as the kicker), the coupling impedance is obtained by the well known formula⁶

$$Z_{hp} = 2 Z_{ref} \frac{(1 - S_{21DUT}/S_{21ref})}{(S_{21DUT}/S_{21ref})}$$

This formula is used by the *hp* network analyzer and is quite useful in an exploratory study involving distributed impedances. However, if accurate results are required, at least the "log-formula" should be used;⁷ although itself an approximation, it is extremely simple to use and sufficient in the present application,

$$Z_{log} = -2 Z_{ref} \ln \frac{S_{21DUT}}{S_{21ref}}$$

The rigorous treatment of distributed impedances and the derivation of the log-formula approximation can be found in the previous report by Hahn *et al.*⁴

⁶H. Hahn and F. Pedersen, Report BNL #50870 (1978).

⁷L. S. Walling, D. E. McMurry, D. V. Neuffer, H. A. Thiessen, Nucl. Instr. Meth., A 281, p. 433 (1989).

III. THE HIGH-FREQUENCY IMPEDANCE OF THE KICKER SYSTEM

The *hp* network analyzer output for the forward scattering coefficient $S_{21\text{DUT}}$ (normalized to $S_{21\text{ref}} = 1$) of the kicker system, i.e. the (half-length) kicker with the Blumlein pulser connected, is shown in Fig. 4. The same data, converted into real and imaginary part of the coupling impedance is shown in Fig. 5. The more exact result for the half-length kicker, obtained by using the log-formula, is given in Table 1 and compared to the *hp*-calculated values. It is seen, that the use of the *hp*-formula can lead to significant errors.

The coupling impedance of the kicker system with one half-length unit, measured without ceramic beam tube, follows in the frequency range from ~ 0.1 to 1 GHz. to be $|Z/n| \leq 0.14$ Ω/ring and less at higher frequencies; the coupling impedance of the hybrid kicker shows no resonances.

These results for the hybrid kicker are essentially the same as for the all-ferrite kicker previously measured⁴ and suggest that the coupling impedance above ~ 100 MHz is completely determined by the ferrite and the beam is decoupled from the Blumlein pulser. This statement is confirmed by two measurements shown in Fig. 6, in which the result for the kicker with the feeding cables disconnected is plotted together with the data from Fig. 5.

Table 1. Longitudinal Coupling Impedance of Injection Kicker System Without Beam Tube

$f(\text{MHz})$	n	$S_{21\text{DUT}}$	Half Length		Ring
			$Z_{\text{hp}} (\Omega)$	$Z_{\text{log}} (\Omega)$	$ Z/n (\Omega)$
100	1279	$0.986 \exp(-j 3.79^\circ)$	$4.06 + j 22.5$	$4.69 + j 21.8$	0.139
300	3837	$0.937 \exp(-j 10.47^\circ)$	$16.5 + j 65.1$	$21.4 + j 60.3$	0.133
600	7673	$0.896 \exp(-j 20.56^\circ)$	$15.0 + j 131.6$	$36.1 + j 118.4$	0.129
900	11510	$0.787 \exp(-j 29.54^\circ)$	$35.5 + j 210.6$	$79.2 + j 170.2$	0.130

31 V. 26.
 sysk 4
 H-185

31. V. 86

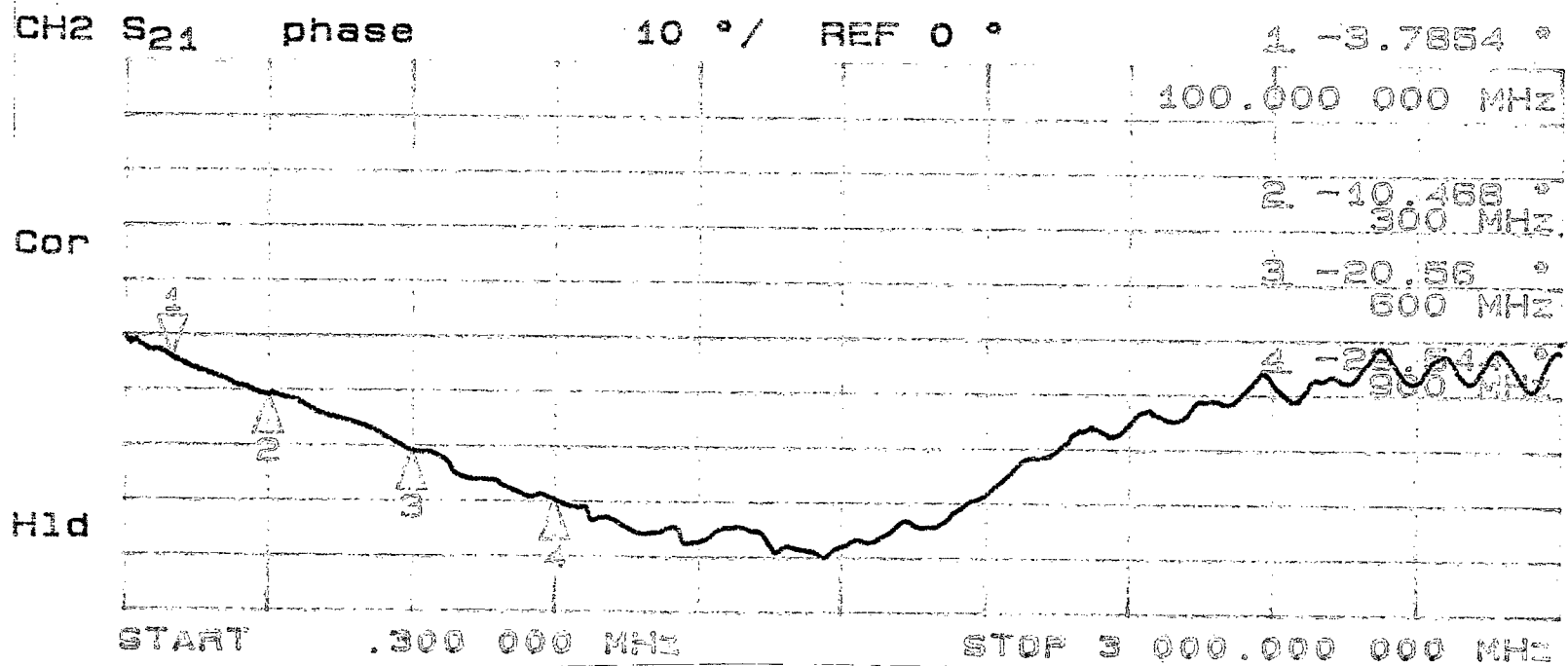
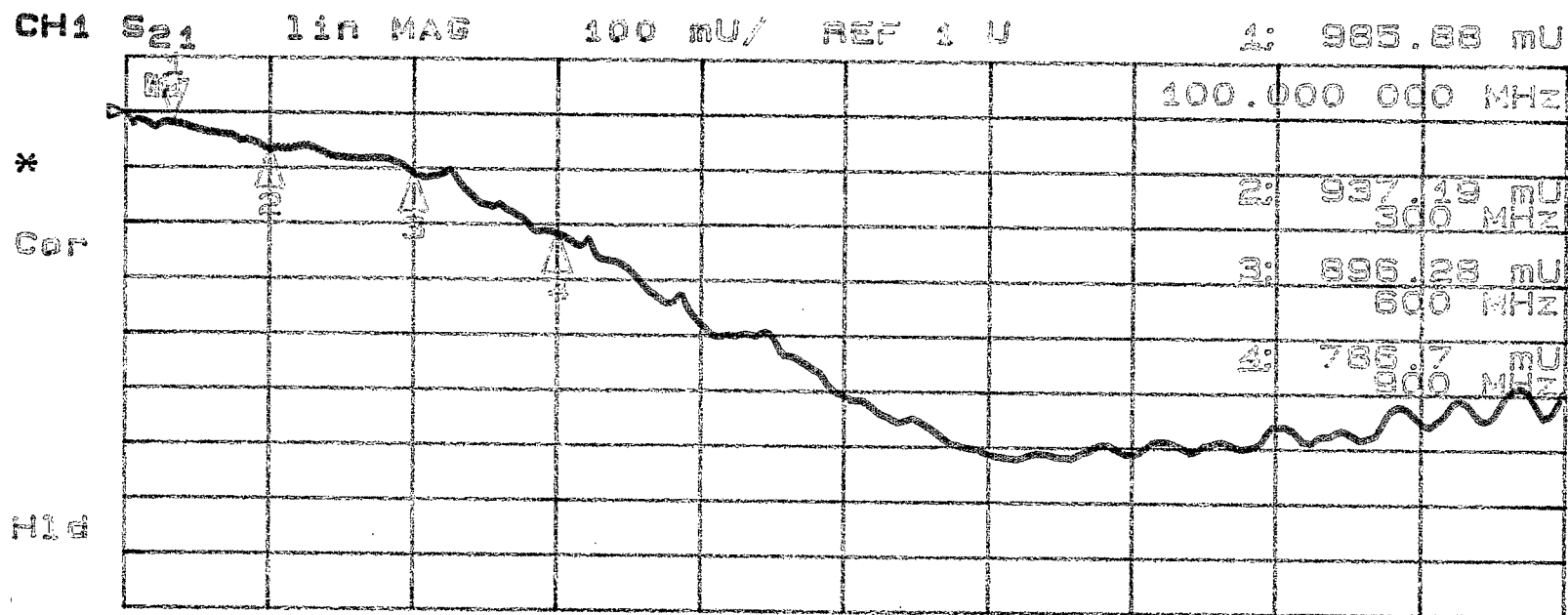


Fig. 4. Forward scattering coefficient of kicker system.

31. V. 96
H-1.85

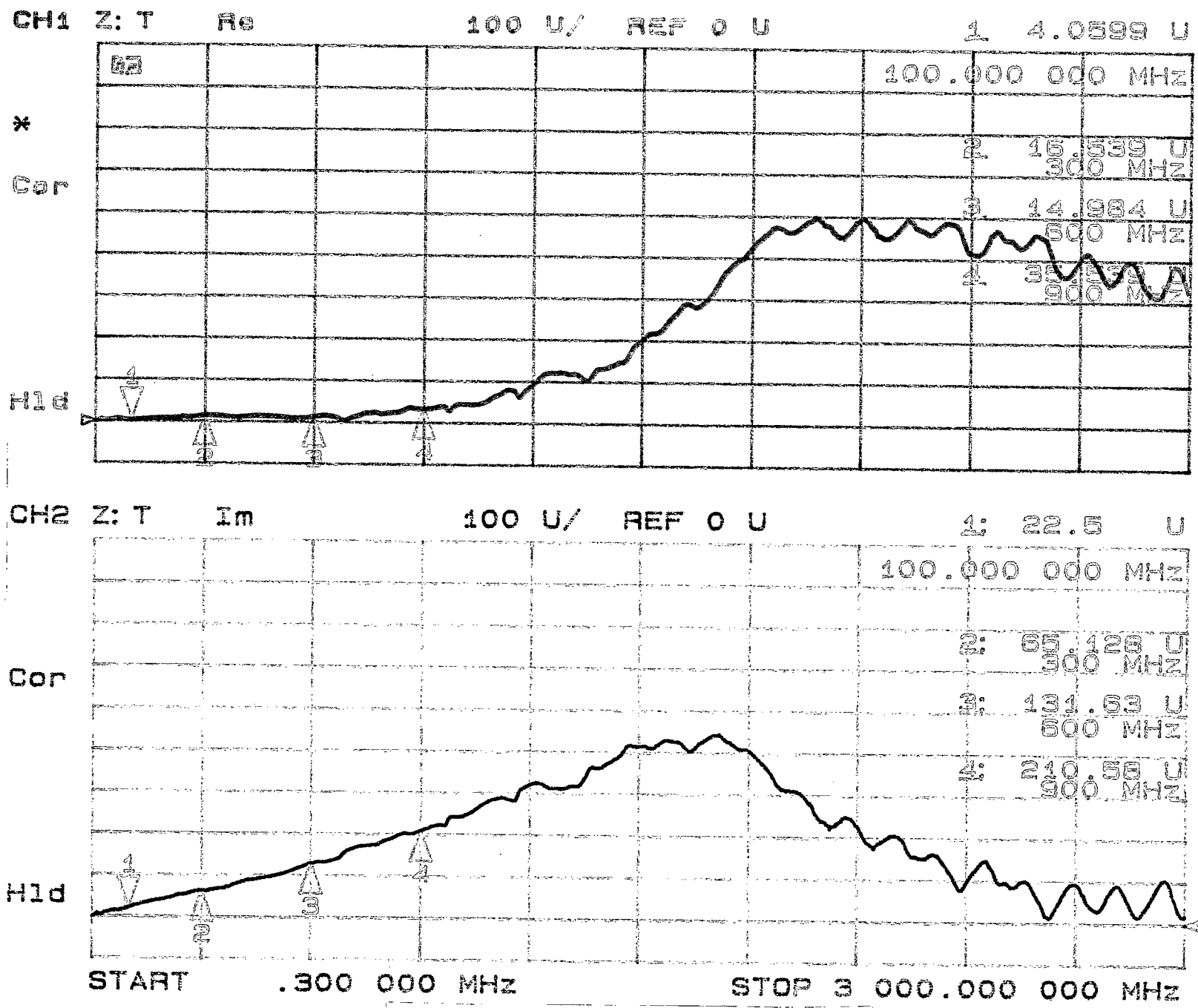


Fig. 5. *hp* coupling impedance of kicker system.

31. V. 96.

System + open
dark shows
open
H-1.85
31. V. 96

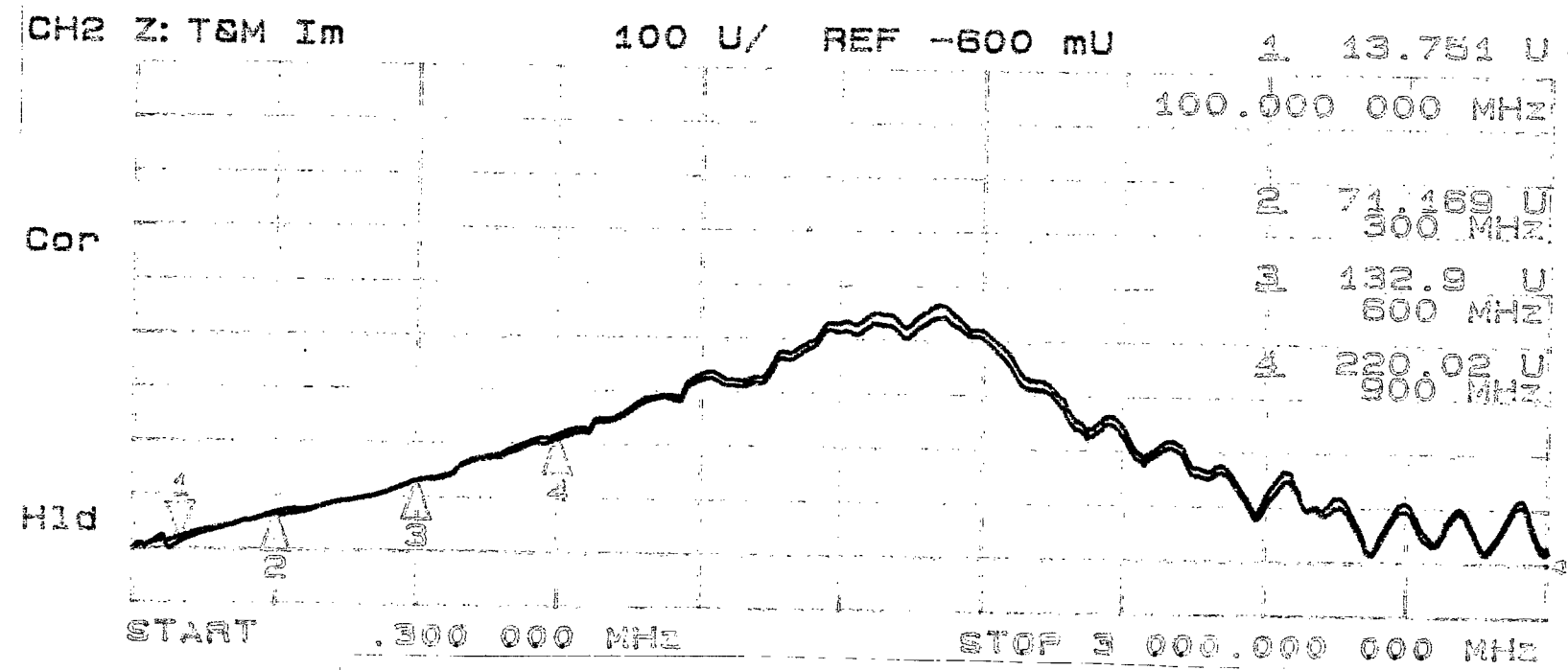
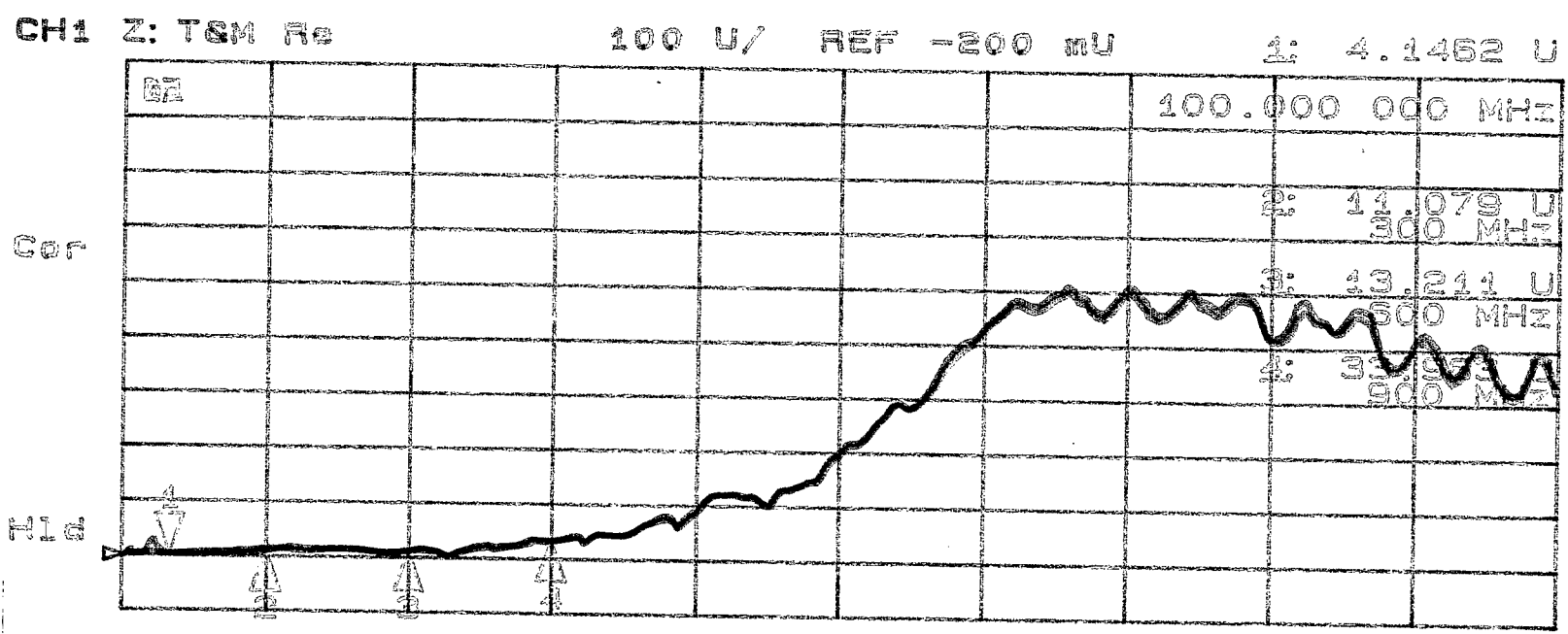


Fig. 6. Impedance comparison of kicker system versus free-standing kicker.

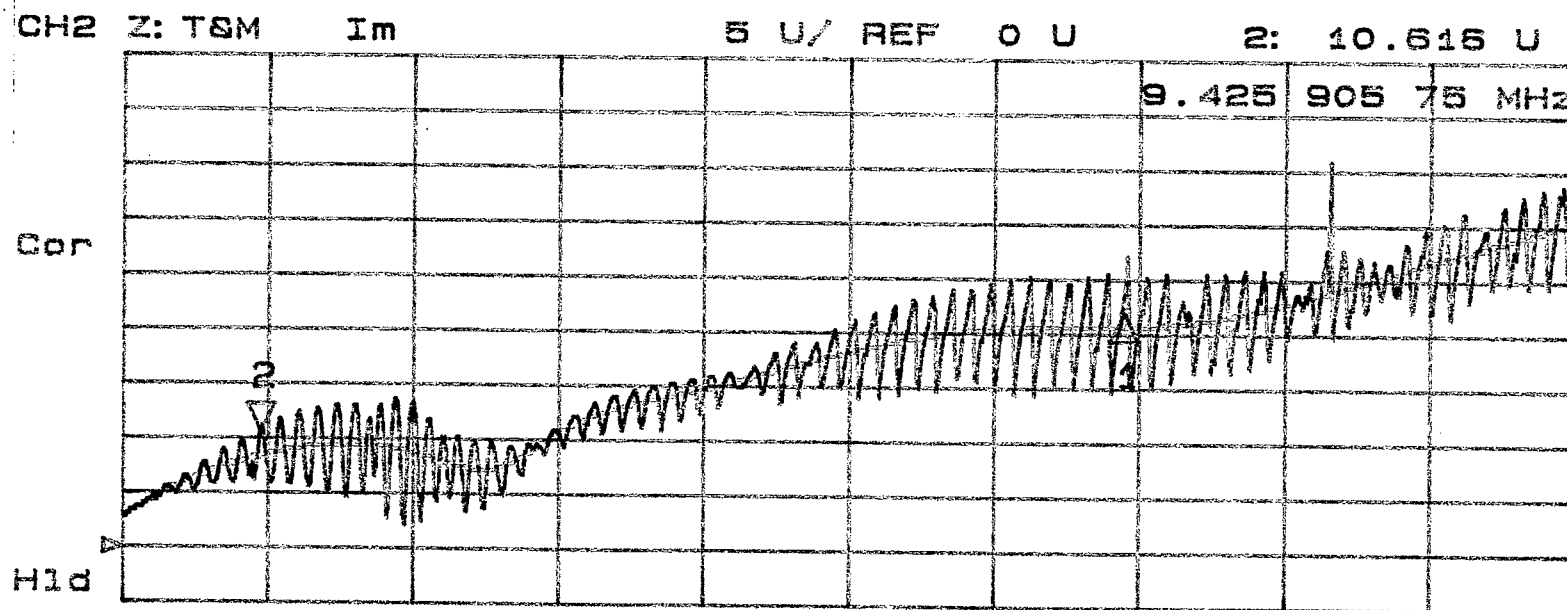
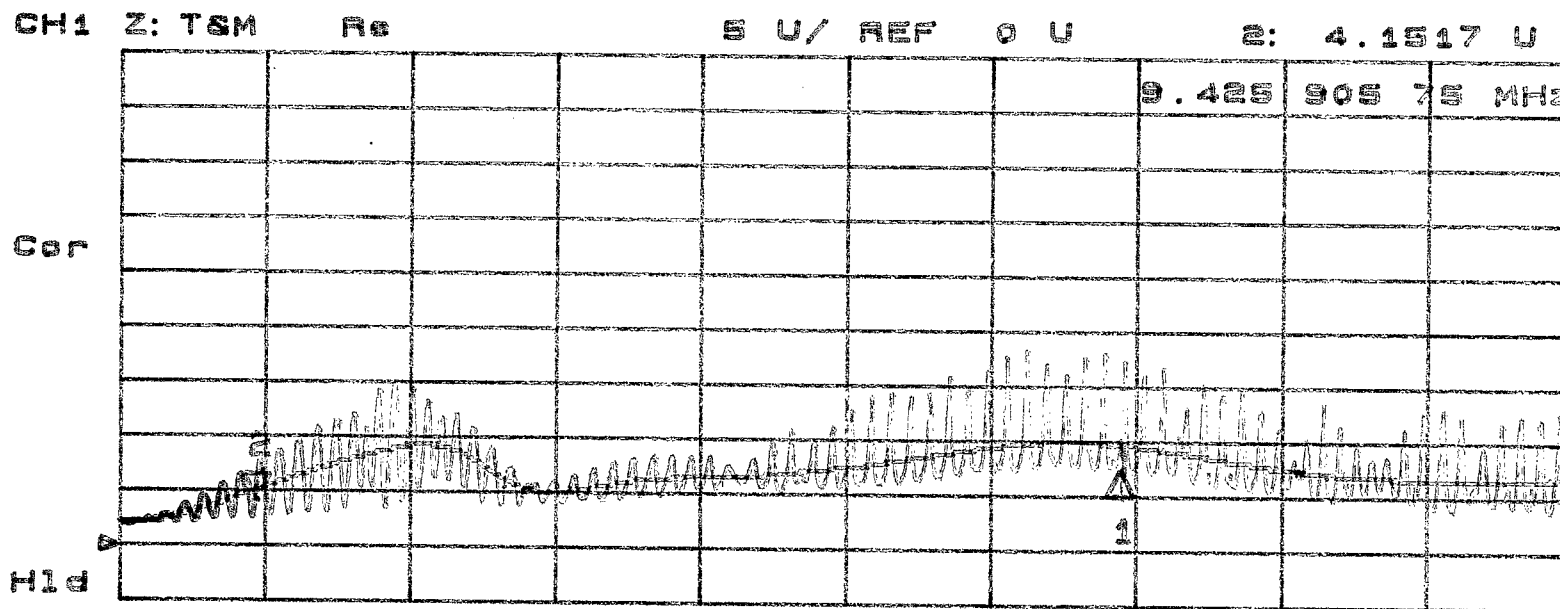
IV. THE LOW-FREQUENCY COUPLING IMPEDANCE OF THE KICKER SYSTEM

At low frequencies, <100 MHz, the ferrite permeability and losses are sufficiently close to ideal that they can be ignored in first approximation. It follows that the kicker is "transformer-coupled" to the beam and the kicker terminations become visible in the coupling impedance.

The measured coupling impedance of the kicker system below 100 MHz is shown in Fig. 7 together with the results - stored in memory - for the free-standing kicker, i.e. with pulser and cables disconnected and replaced by a matched termination. The smooth curve represents the free-standing kicker. The rapid oscillation of the impedance are due to the ~ 75 m long cables between kicker and Blumlein pulser.

Although visible, the contributions from pulser and connecting cables do not require the addition of a saturating inductor (D.I.S.I.).⁸ The presence of a saturating inductor would smooth the curve, but since it is done at the peak values, it effectively maintains the impedance. In fact, the saturating inductor acts in the limit as an "open" terminal, and the impedance could become larger as seen from the impedance curve in Fig. 8 for the kicker with load end matched and the input end open. The losses of the long cable provide a partial matching and thus lower coupling impedance peaks.

⁸H. J. Tran, M. J. Barnes, G. D. Wait, Y. Yan, Proc. 1993 PAC, Washington, vol. 5, p. 3402.



START 1 KHz

STOP 100 MHz

Fig. 7. Coupling impedance and low frequencies of kicker system (rapid oscillation) and free-standing kicker (smooth curve).

31. V. 96
 system +
 both ends
 terminated
 H-185
 31. V. 91

3. V: 86
 OPEN
 "H-1.85"

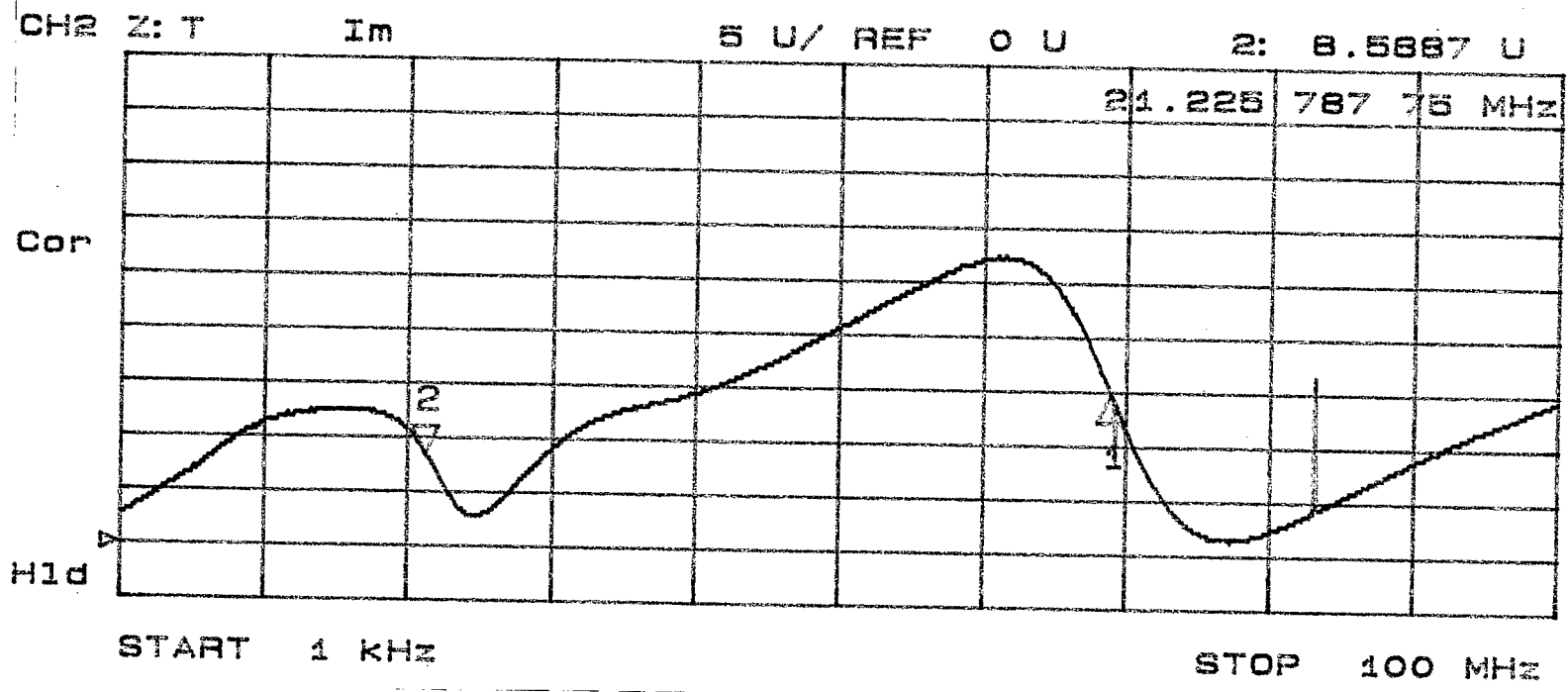
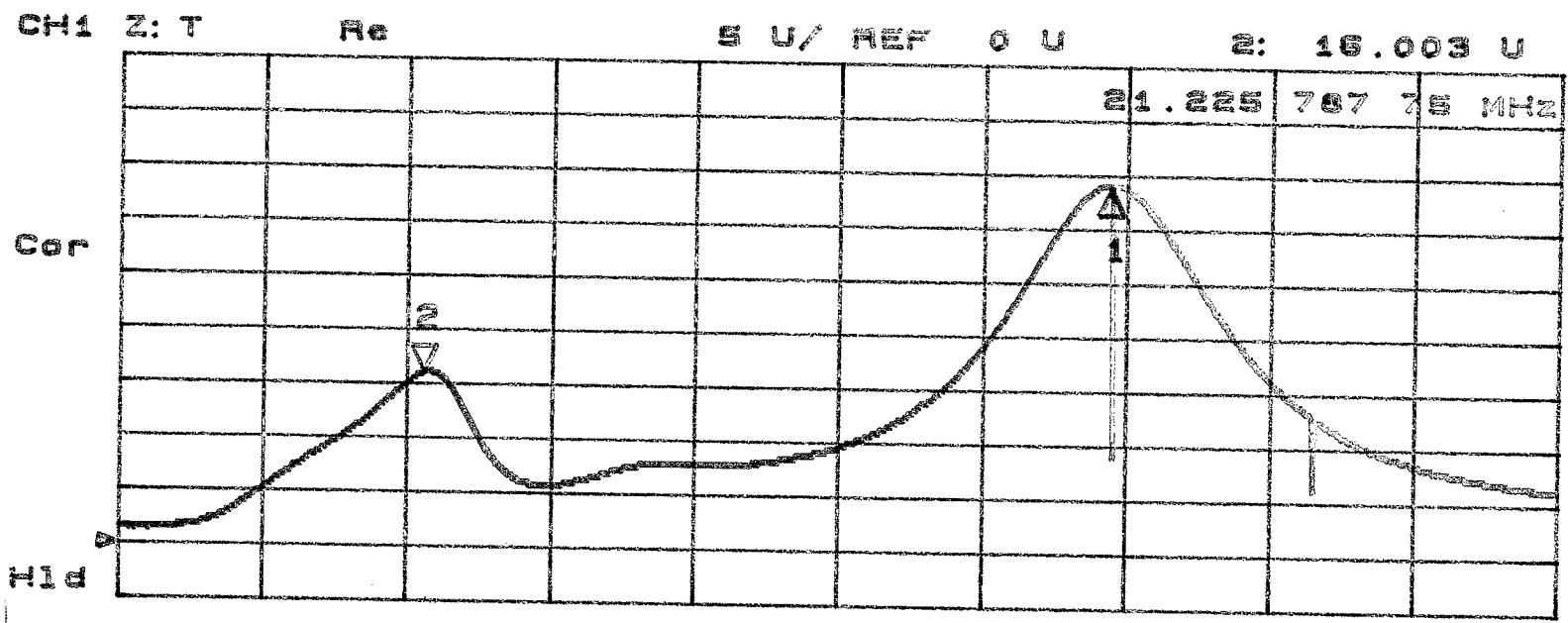


Fig. 8. Low frequency coupling impedance of kicker with open input.

V. THE KICKER WITH CERAMIC BEAM TUBE

1. The Kicker with Beam Tube

The kicker will be operated in air and requires a ceramic beam tube, the dimensions of which are 47.6 mm o.d. and 41.3 mm i.d. Insertion of the uncoated ceramic beam tube into the kicker increases the capacity by 2% (9 pF in 797 pF), and decreases the characteristic impedance by 1% to 27.5 Ω .

The coupling impedance of the kicker plus beam tube assembly was measured with input and output terminated. The forward scattering coefficient and the hp impedance are shown in Figs. 9 and 10. Note that the hp formula leads to qualitatively wrong results (i.e., negative real part of the impedance), whereas the log formula is correct as seen from the data in Table 2.

Table 2. Longitudinal Coupling Impedance of Injection Kicker System With Beam Tube

f/MHz	n	$S_{21\text{DUT}}$	Half Length		Ring
			$Z_{hp}(\Omega)$	$Z_{\log}(\Omega)$	$ Z/n (\Omega)$
100	1279	$0.974 \exp(-6.50^\circ)$	$6.59 + j 39.0$	$8.54 + j 37.4$	0.24
300	3837	$0.948 \exp(-15.57^\circ)$	$5.41 + j 95.1$	$17.6 + j 89.7$	0.19
600	7673	$0.889 \exp(-34.07^\circ)$	$-23.0 + j 211.6$	$38.7 + j 196.2$	0.22
900	11510	$0.081 \exp(-52.14^\circ)$	$-78.5 + j 331.3$	$73.4 + j 300.3$	0.21

In summary, the longitudinal coupling impedance of the injection kicker with uncoated ceramic beam tube is in one ring of the collider

$$\frac{Z}{n} \leq 0.22 \text{ } \Omega/\text{ring}$$

in the frequency range from 0.1 to 1 GHz, but lower at higher frequencies and is free of resonances in the measured region up to 3 GHz.

Overall, one finds that the impedance contribution by the injection kicker is tolerable without the need for special impedance reduction measures such as a low-impedance (R -square, $R_{sq} \sim 1\text{-}10\ \Omega$) coating. A low-impedance coating can limit the rise time and cause arcing at higher fields. The time constant of the magnetic field due to the eddy currents in the coating is given by

$$T_E = \frac{1}{2} \mu_o \frac{b}{R_{sq}} = \frac{\mu_o}{4\pi \langle R \rangle}$$

with $\langle R \rangle$ the beam tube resistance per unit length. It is seen that a coating with $R_{sq} > 10\ \Omega$ will not lengthen the field rise time by more than ~ 1 nsec. In practice, however, the use of a full low-impedance coating is prevented by sparking during pulses (as observed on the kicker).

A high-resistance coating ($R_{sq} \sim 10\text{-}100\ \text{k}\Omega$) will not reduce the coupling impedance but is required to prevent electrostatic charging of the beam tube, and will be provided in the RHIC kicker.

CH1 S₂₁ 11n MAG 200 mU/ REF 1 U

1 974.43 mU
100.000 000 MHz

*

Cor

1

2

3

4

2 948.03 mU
300 MHz

3 889.28 mU
600 MHz

4 800.63 mU
900 MHz

H1d

CH2 S₂₁ phase

20 °/ REF 0 °

1: -6.5017 °

100.000 000 MHz

Cor

1

2

3

4

2: -15.559 °
300 MHz

3: -34.07 °
600 MHz

4: -52.144 °
900 MHz

H1d

START

.300 000 MHz

STOP 3 000.000 000 MHz

Fig. 9. Forward scattering coefficient of kicker with ceramic beam tube.

is clear with ~~the~~ tube
kicker in line

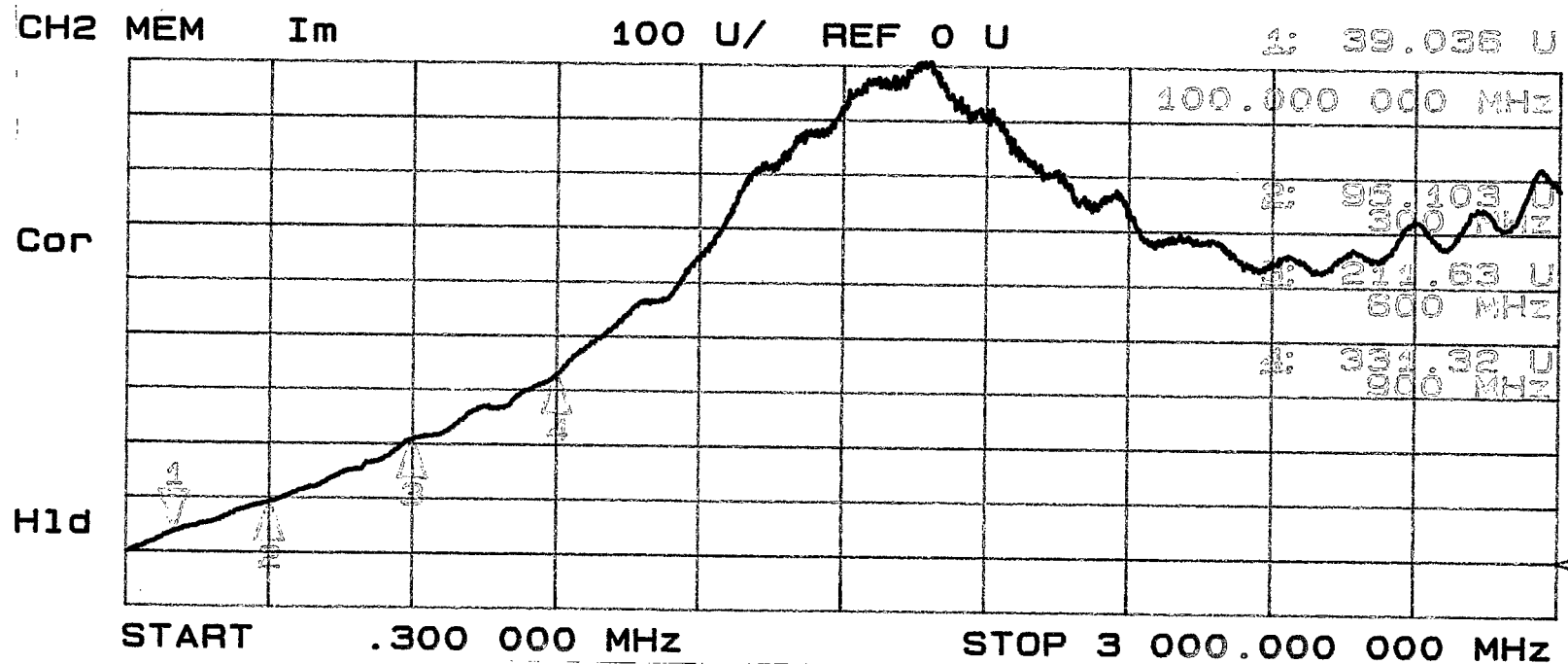
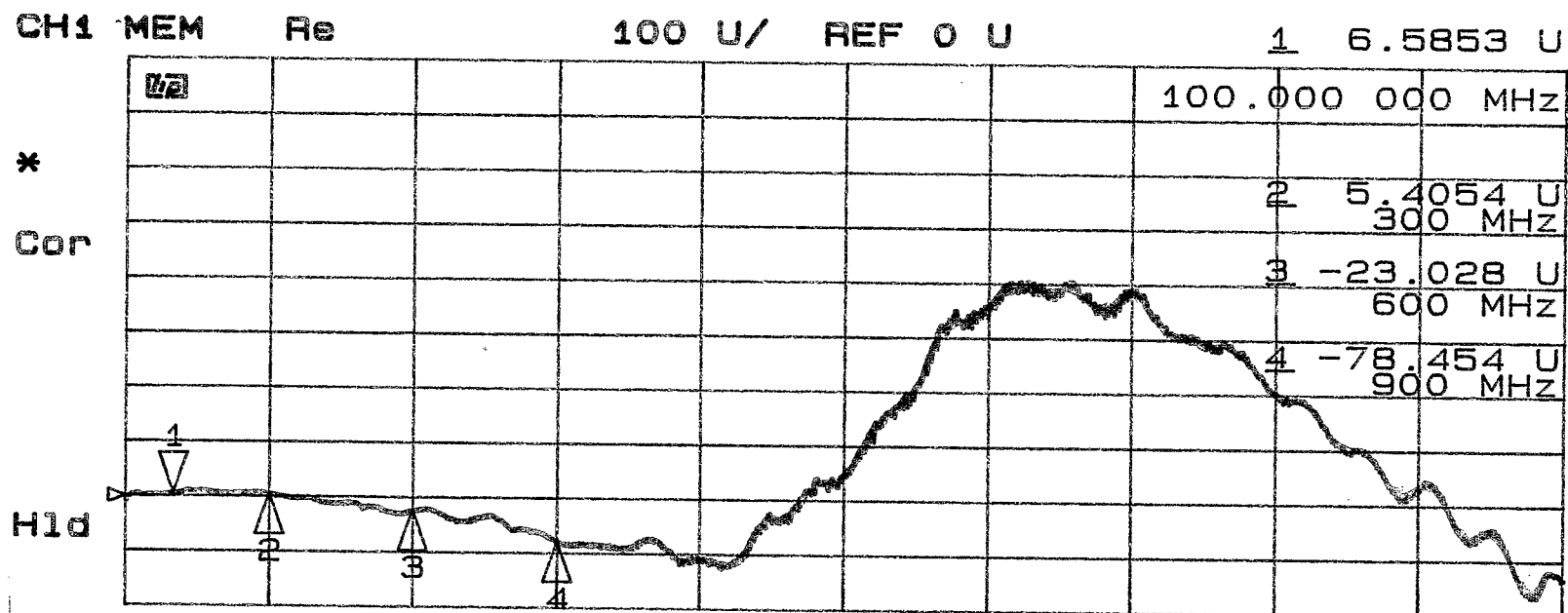


Fig. 10. *hp* coupling impedance of kicker with beam tube.

2. The Ceramic Beam Tube

The hp impedance of the kicker with and without beam tube is shown together in Fig. 11. The contribution of the ceramic beam tube to the kicker impedance is significant and deserves a more detailed study. A theoretical estimate of the kicker impedance with uncoated beam tube is derived in the Appendix. It is shown that, at sufficiently low frequencies, the total coupling impedance is simply the sum of the kicker impedance without beam tube plus that of the beam tube alone. In order to verify this result, measurements on the beam tube alone were made.

The coupling impedance of the uncoated ceramic beam tube, alone without kicker, was measured in the test set up. The scattering coefficient and the hp impedance are shown in Figs. 12 and 13, respectively. The coupling impedance of the half-length ceramic tube alone is at “low” frequencies $Z/n \approx 14 \text{ m}\Omega$, corresponding to $Z/n = 0.11 \text{ }\Omega/\text{ring}$.

It is instructive to compare the measured results with the calculated estimates from the simple model of a coaxial arrangement of center conductor, ceramic beam tube and perfect outer conductor.^{9, 10} The coupling impedance, in the extreme-relativistic, long-wavelength limit can be estimated from the expression

$$\frac{Z}{n} = j \frac{Z_0 l_B}{2\pi R} \left(1 - \frac{1}{\epsilon} \right) \ln \frac{r_D}{r_B}$$

with $\epsilon \approx 10$, $l_B = 0.661 \text{ m}$, $2\pi R = 3834 \text{ m}$, $r_D = 23.8 \text{ mm}$, and $r_B = 20.6$ to be $Z/n \approx 8 \text{ m}\Omega$, a factor of <2 below the measured result. This discrepancy is outside of the measuring accuracy and has not yet been identified; geometrically differences between model and test setup, especially the off-axis location of the center conductor and effects at the beam tube ends, are suspected.

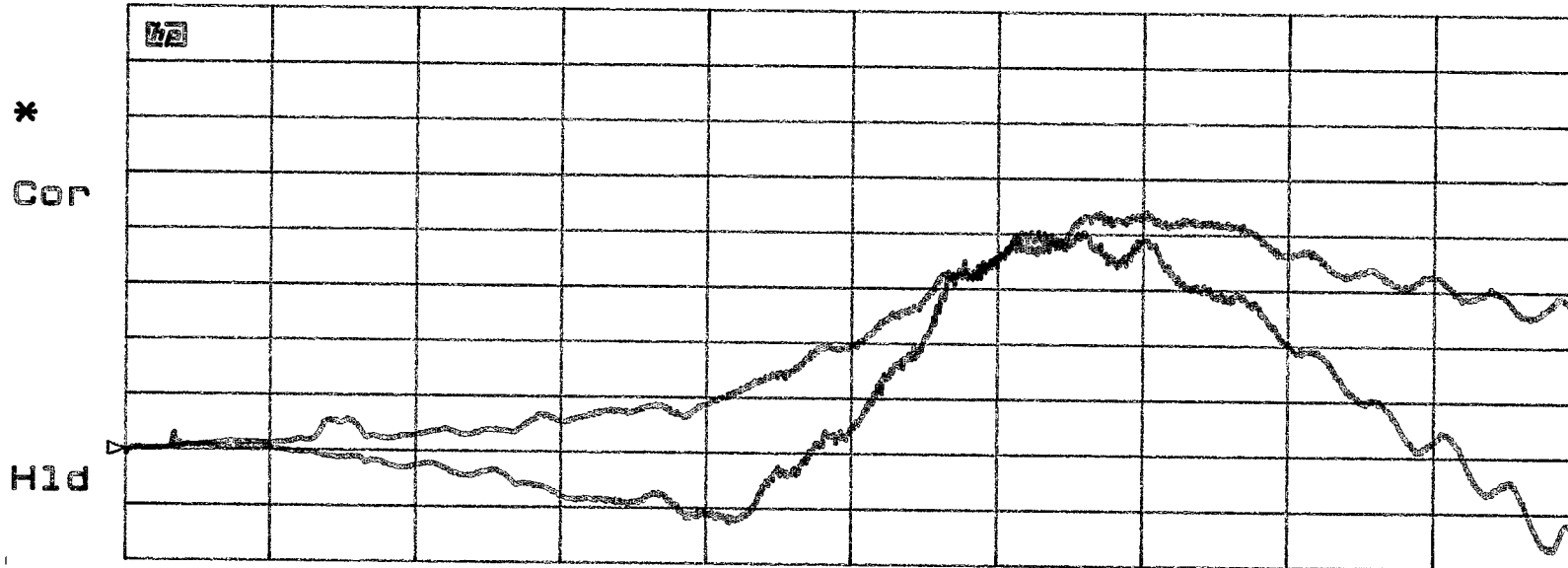
The hp impedances of coated beam tubes are compared with those of the uncoated tubes in Figs. 14 and 15. The impedance of the tube with $R_{sq} \sim 1 \text{ k}\Omega$ is essentially unchanged. The low impedance coating ($R_{sq} \sim 1 \text{ }\Omega$) shorts the beam tube impedance completely. (The ungrounded coating shows weak $\lambda/2$ resonances at a multiple of $\sim 110 \text{ MHz}$.)

⁹B. Zotter, Particle Accelerators, Vol. 1, p. 311 (1970).

¹⁰S. S. Kurennoy, Proc. 1993 Part. Acc. Conf., Washington, D.C., Vol. 5, p. 3420 (1993).

CH1 Z: T&M Re

100 U/ REF 0 U



CH2 Z: T&M Im

100 U/ REF 0 U

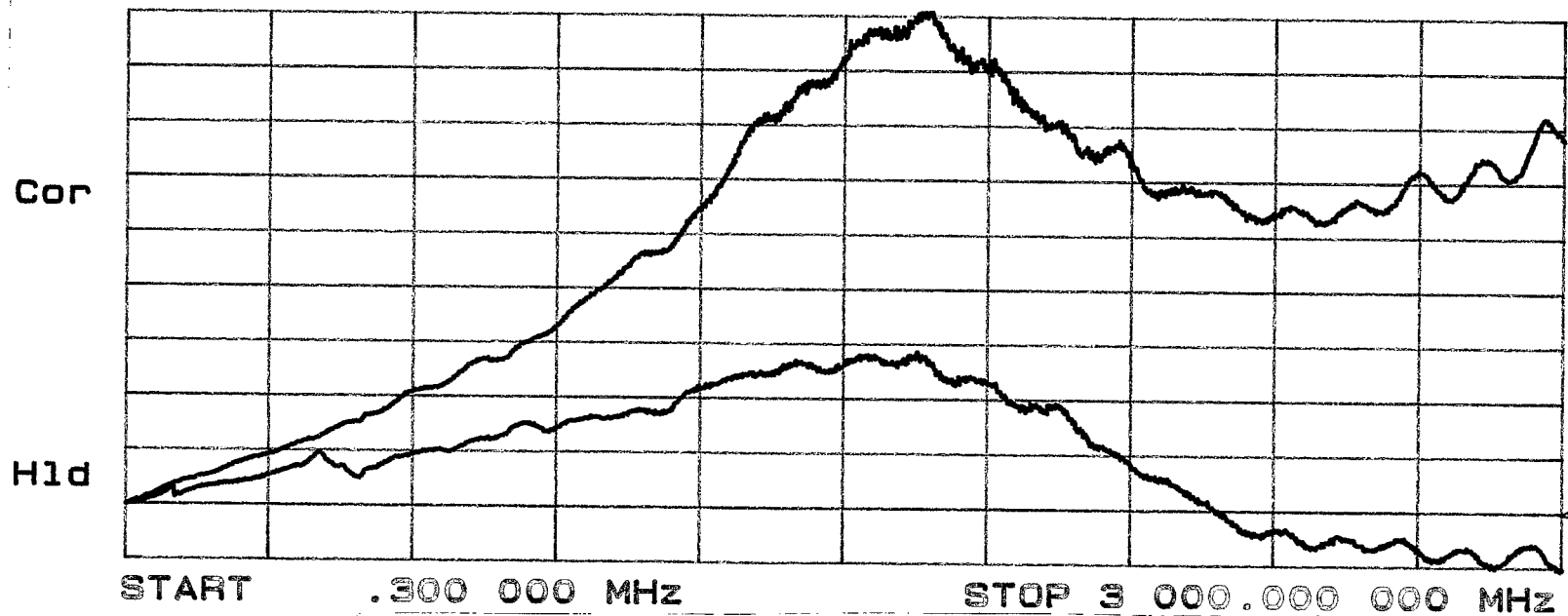


Fig. 11. Comparison of impedance of kicker with and without beam tube.

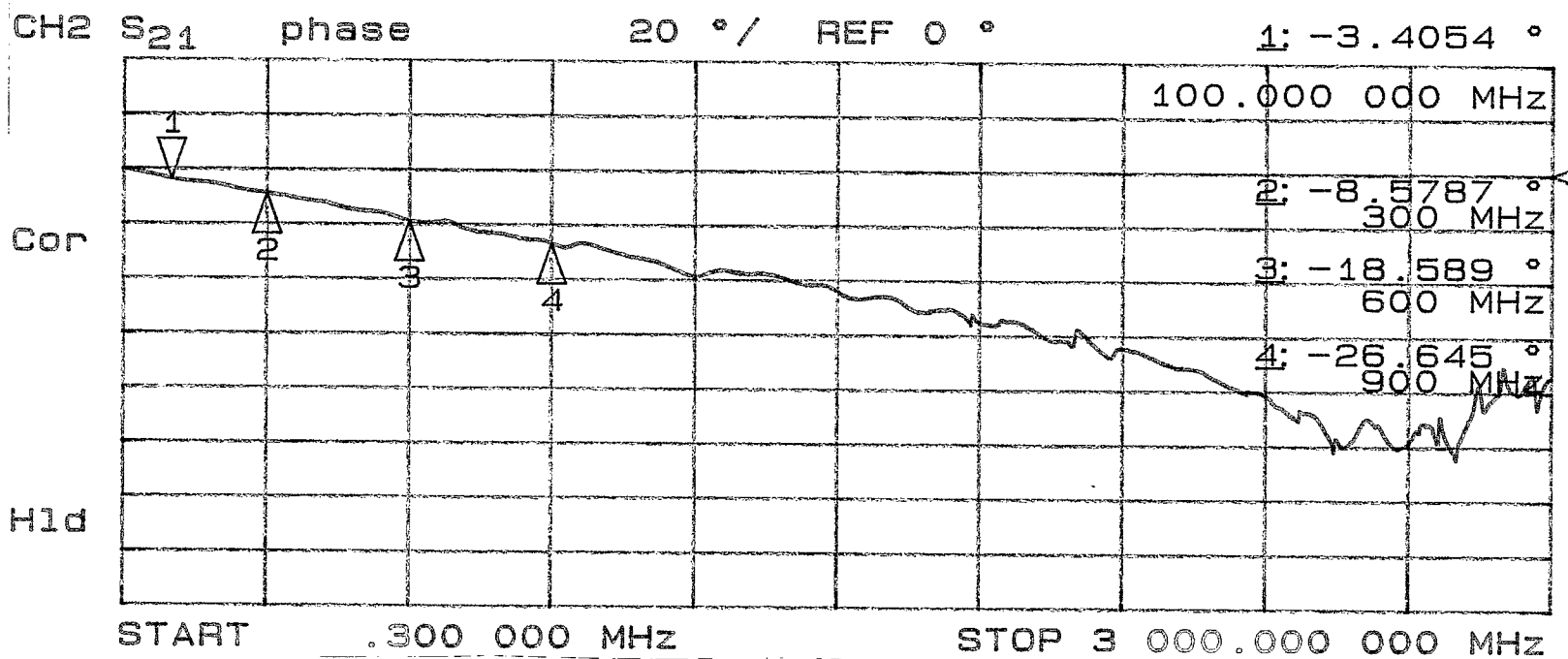
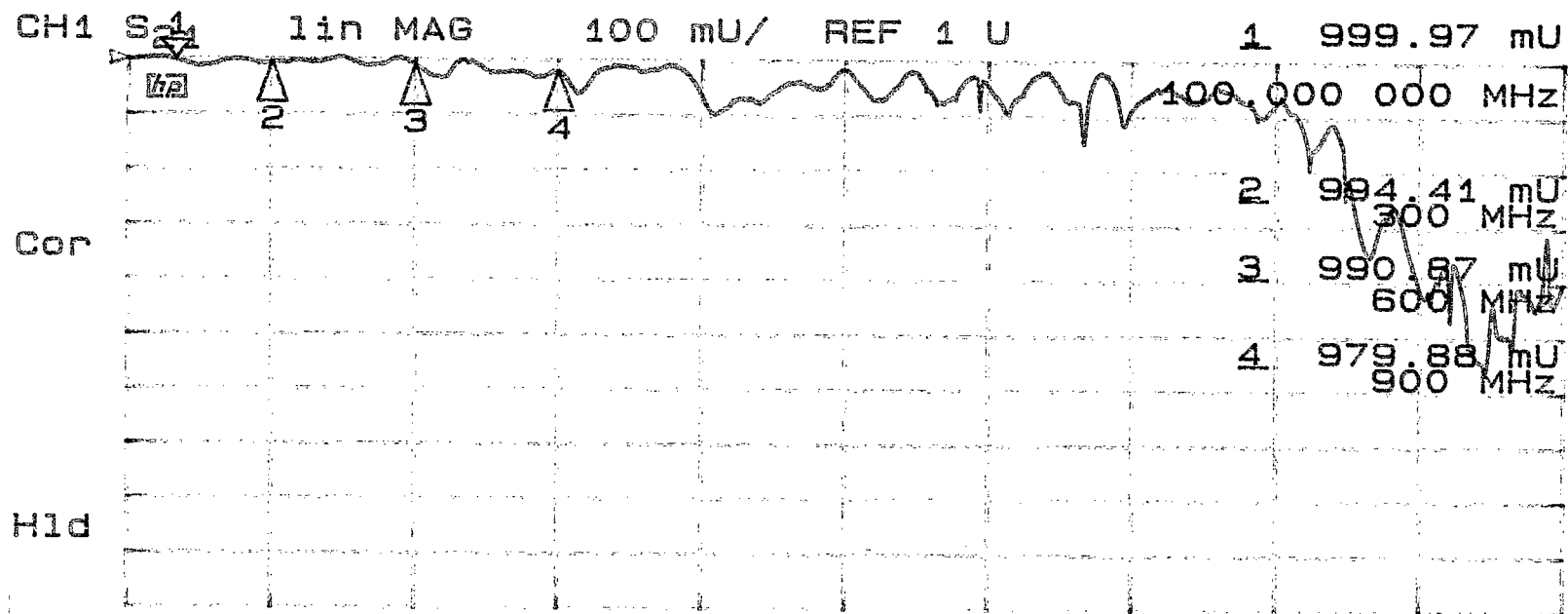


Fig. 12. Forward scattering coefficient of uncoated ceramic beam tube.

Tube uncoated

66.1 cm

July 1

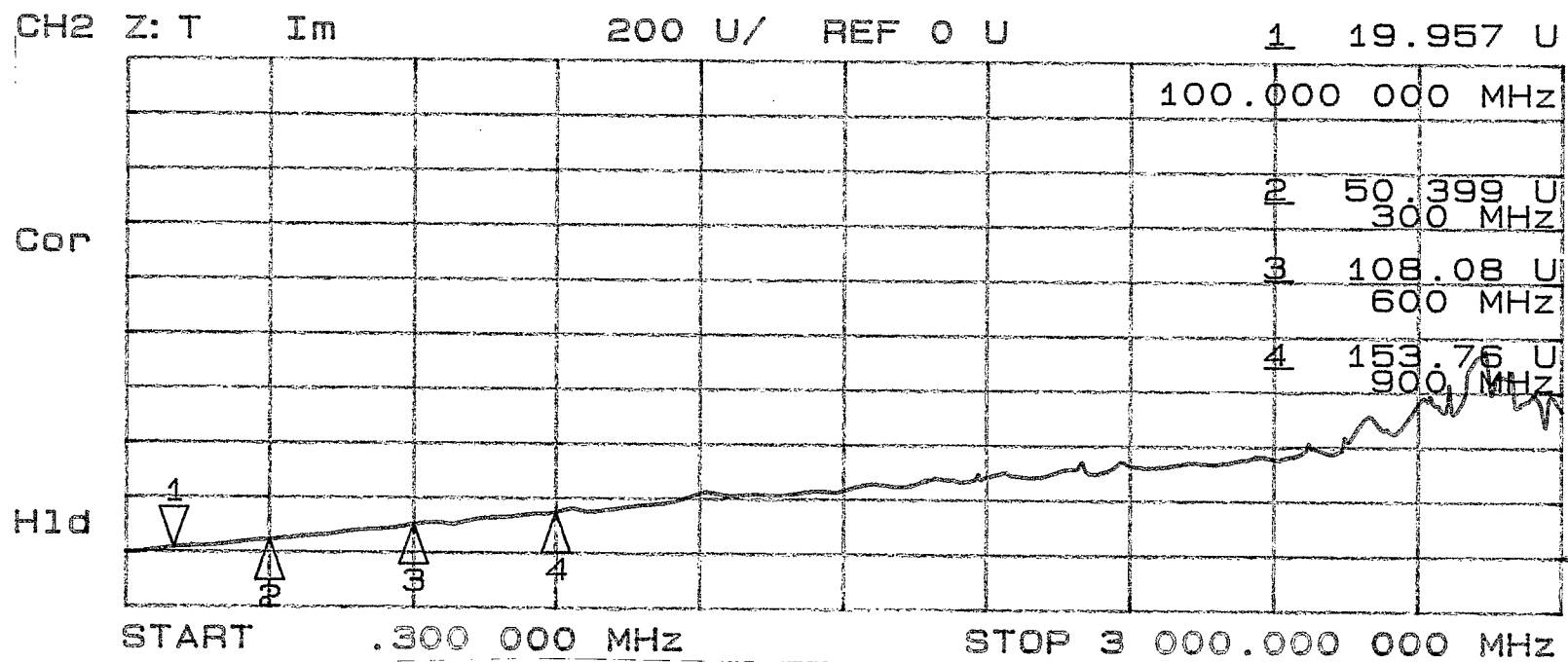
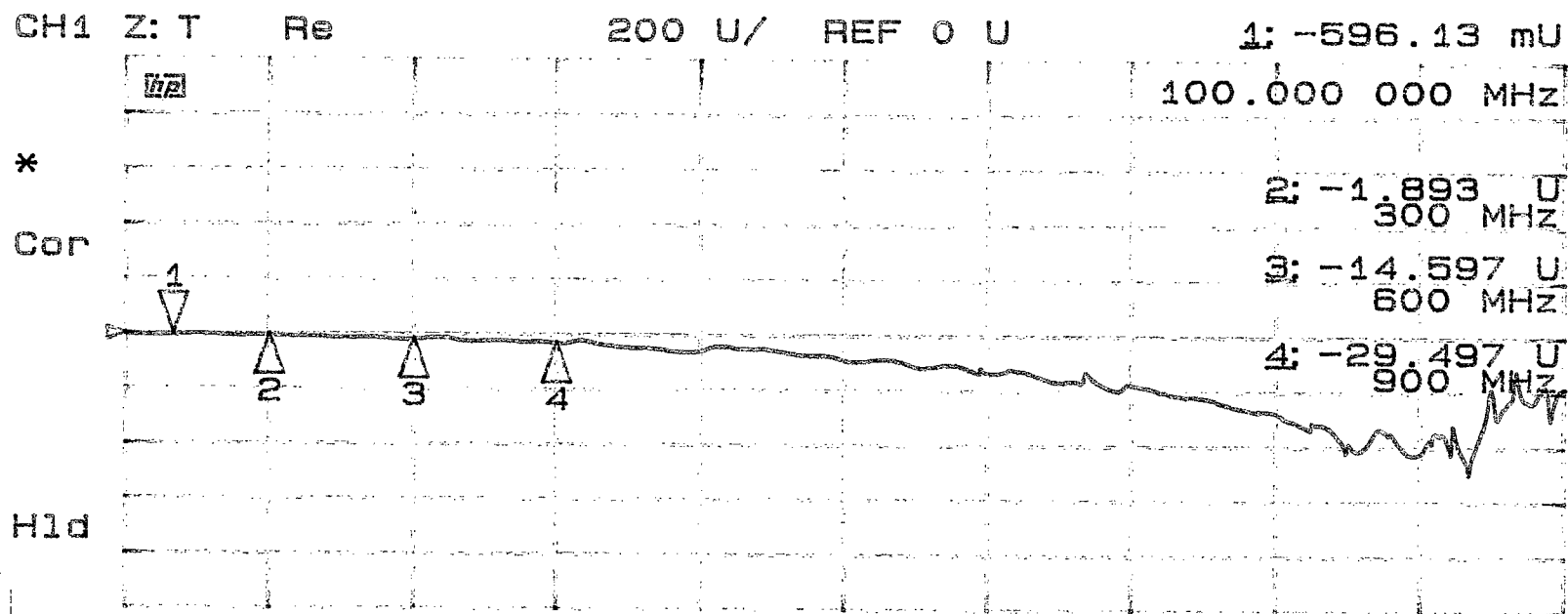


Fig. 13. *hp* coupling impedance of uncoated ceramic beam tube.

Tube uncoated

July 1

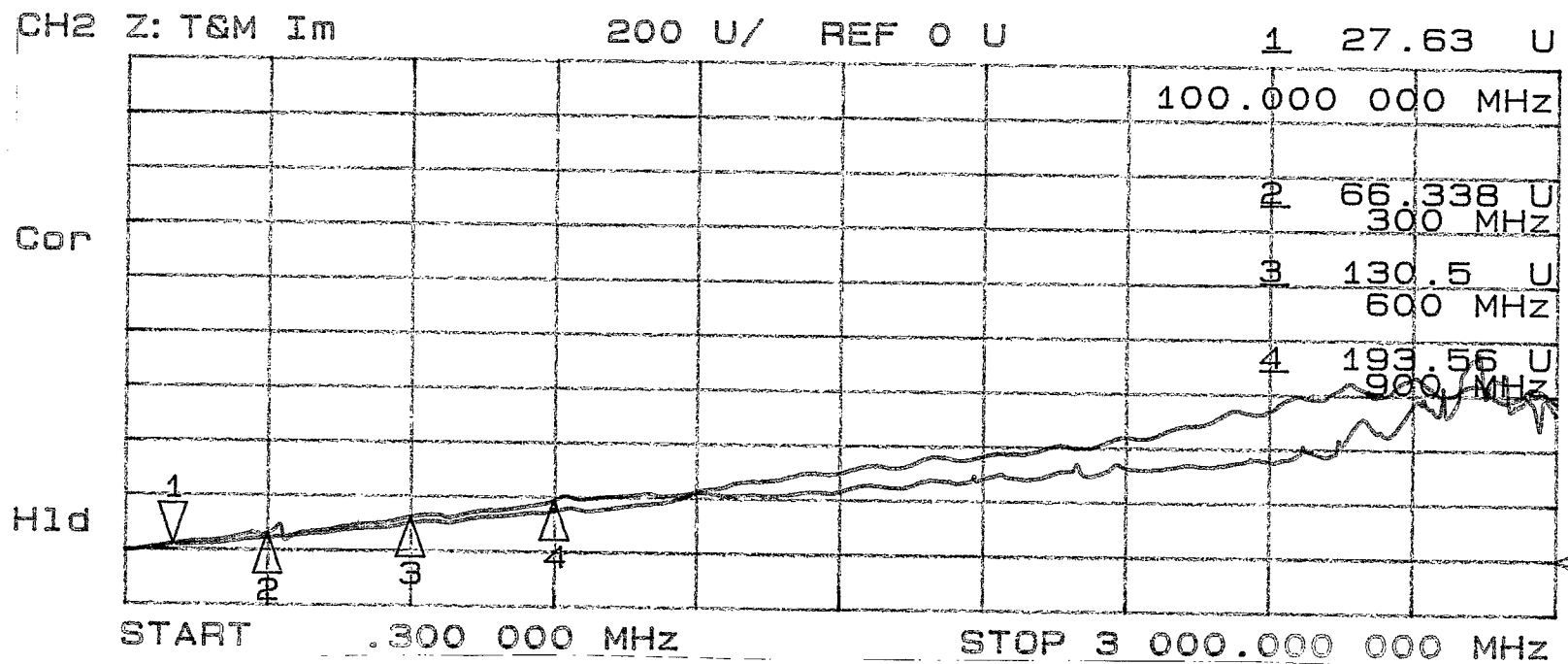
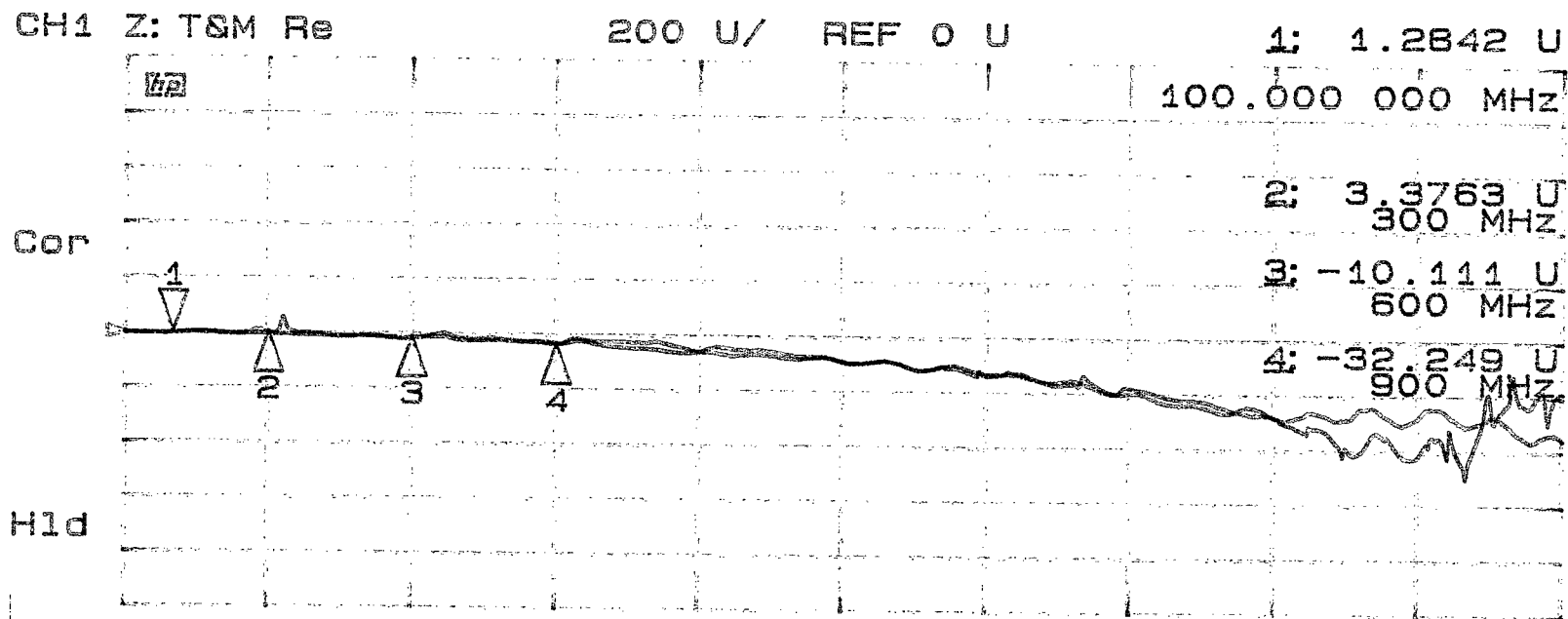


Fig. 14. *hp* impedance of beam tube with $R_{sq} \sim 1 \text{ k}\Omega$ coating versus uncoated tube.

SKR vs uncoated Tube
Data for SKR

60.5 GHz
1.7.7.14

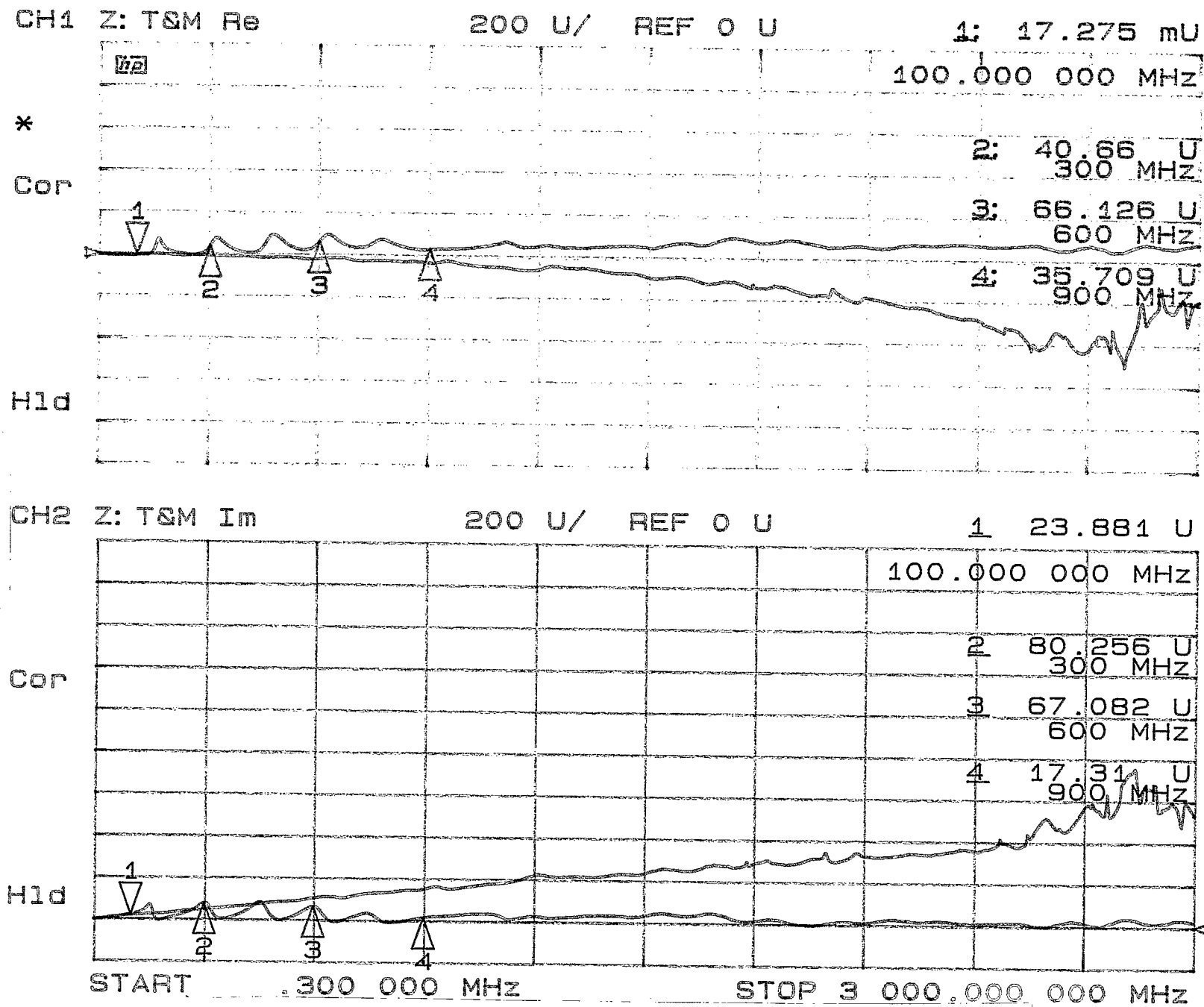


Fig. 15. h_p impedance of beam tube with $R_{sq} \sim 1 \Omega$ coating versus uncoated tube.

5L vs uncoated
for 5L

1.7u1-

APPENDIX: THEORETICAL COUPLING IMPEDANCE OF KICKER WITH BEAM TUBE

A theoretical estimate of the longitudinal coupling impedance of a kicker with coated ceramic beam tube can be derived from the simplified model of a structure with concentric circular elements as shown in Fig. 16.

Relevant results for this type of geometry were previously published by Zotter⁹ and Piwinski¹¹ and are quoted by Kurennoy.¹⁰ However, no explicit expression for the coupling impedance of the kicker with coated ceramic tube could be found, and the need for its derivation remained.

The expressions for the fields of interest, assumed to be rotational symmetric, within a region with uniform properties are given by (in natural units $c = \mu_0 = 1$)

$$E_z \sim j \frac{1}{\omega} \{ c_k \kappa^2 K_0(\kappa r) + c_I I_0(\kappa r) \}$$

$$H_\varphi \sim \epsilon \left\{ c_k \kappa K_1(\kappa r) - c_I \frac{I_1(\kappa r)}{\kappa} \right\}$$

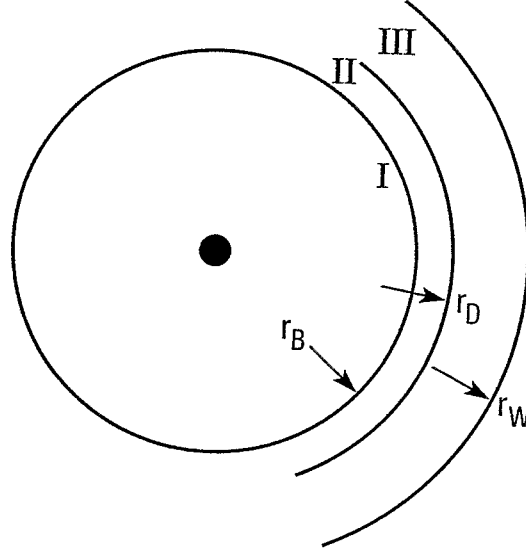


Fig. 16. Kicker model for coupling impedance estimate.

¹¹A. Piwinski, Proc. Trans. IEEE NS-24, p. 1364 (1977).

with the common factor $e^{-j\kappa z} e^{j\omega t}$ suppressed, $I_0(\kappa r)$ and $K_0(\kappa r)$ the modified Bessel functions, and

$$\begin{aligned}\omega &= v v \\ \kappa^2 &= (v^2 - \epsilon)\omega^2\end{aligned}$$

The use of matrix notation considerably simplifies the treatment of a structure with regions of different dielectric properties. The fields at the inner and outer radius of a region are related by the matrix

$$\begin{bmatrix} E_z(r_i) \\ H_\phi(r_i) \end{bmatrix} = \begin{bmatrix} M_{ee} & M_{eh} \\ M_{he} & M_{hh} \end{bmatrix} \begin{bmatrix} E_z(r_o) \\ H_\phi(r_o) \end{bmatrix}$$

with the rigorous expressions for the matrix elements

$$\begin{aligned}M_{ee} &= \kappa r_o [I_0(\kappa r_i) K_1(\kappa r_o) + I_1(\kappa r_o) K_0(\kappa r_i)] \\ M_{eh} &= j \frac{\kappa}{\epsilon \omega K_1(\kappa r_o)} \{K_0(\kappa r_i) - \kappa r_o [I_0(\kappa r_i) K_1(\kappa r_o) + I_1(\kappa r_o) K_0(\kappa r_i)] K_0(\kappa r_o)\} \\ M_{he} &= j \frac{\epsilon \omega}{I_0(\kappa r_o)} \left\{ \frac{I_1(\kappa r_i)}{\kappa} - \kappa r_o [I_0(\kappa r_o) K_1(\kappa r_i) + I_1(\kappa r_i) K_0(\kappa r_o)] \frac{I_1(\kappa r_o)}{\kappa} \right\} \\ M_{hh} &= \kappa r_o [I_0(\kappa r_o) K_1(\kappa r_i) + I_1(\kappa r_i) K_0(\kappa r_o)]\end{aligned}$$

Here, only the long-wavelength limit; i.e., $\kappa r \ll 1$, is of interest, whence follows for the ceramic beam tube region

$$\begin{aligned}M_{ee}^{II} &\approx 1 + \frac{1}{4} \kappa^2 r_B^2 \left[1 + \frac{r_D^2}{r_B^2} \left(2 \ln \frac{r_D}{r_B} - 1 \right) \right] \\ M_{eh}^{II} &\approx j \frac{\kappa^2 r_D}{\epsilon \omega} \ln \frac{r_D}{r_B} \\ M_{he}^{II} &\approx -j \frac{\epsilon \omega (r_D^2 - r_B^2)}{2 r_B} + j \frac{\epsilon \omega \kappa^2 r_B^3}{16} \left[1 + \frac{r_D^2}{r_B^2} \left(4 \ln \frac{r_D}{r_B} - \frac{r_D^2}{r_B^2} \right) \right] \\ M_{hh}^{II} &\approx \frac{r_D}{r_B} \left\{ 1 + \frac{1}{4} \kappa^2 r_D^2 \left[1 - \frac{r_B^2}{r_D^2} \left(2 \ln \frac{r_D}{r_B} + 1 \right) \right] \right\}\end{aligned}$$

If, in addition to the long-wavelength limit, one assumes extreme relativistic beams, then

$$\kappa^2 = (1-\epsilon)\omega^2$$

In the long-wavelength, extreme-relativistic approximation the matrix elements outside of the beam tube follow as

$$\begin{aligned} M_{ee}^{III} &\approx 1; & M_{eh}^{III} &\approx 0 \\ M_{he}^{III} &\approx -j \frac{\omega(r_W^2 - r_D^2)}{2r_D}; & M_{hh}^{III} &\approx \frac{r_W}{r_D} \end{aligned}$$

Furthermore, the matrix elements of the coating with surface resistance R_{sq} are

$$\begin{aligned} M_{ee}^I &= 1; & M_{eh}^I &= 0 \\ M_{eh}^I &= -1/R_{sq}; & M_{hh}^I &= 1 \end{aligned}$$

The total matrix representing coating, beam tube and space to an external wall or the kicker is obtained by the matrix product

$$M = M^I M^{II} M^{III}$$

Since the matrix relates electric and magnetic fields rather than voltage and current, its determinant is not unity but

$$\det(M) = r_W/r_B$$

Taking into account the surface impedance (or R -square) definition at r_W

$$\frac{E_z}{H_\phi} = -R_K = -2\pi r_W \frac{Z_{K0}}{l_K}$$

one obtains the measurable coupling impedance of the “device under test” from

$$Z_{DUT} = \frac{l_K}{2\pi r_B} \frac{R_K M_{ee} - M_{eh}}{M_{hh} - R_K M_{he}}$$

The matrix elements to first order in ω are

$$\begin{aligned} M_{ee} &\sim 1 + \dots \\ M_{eh} &\sim -j\omega r_W \left(1 - \frac{1}{\epsilon}\right) \ln \frac{r_D}{r_B} + \dots \\ M_{he} &\sim -\frac{1}{R_{sq}} - j\omega r_B \left(\frac{r_W^2 - r_D^2}{r_B^2} + \epsilon \frac{r_D^2 - r_B^2}{r_B^2} \right) + \dots \\ M_{hh} &\sim \frac{r_W}{r_B} + j \frac{\omega r_W}{R_{sq}} \left(1 - \frac{1}{\epsilon}\right) \ln \frac{r_D}{r_B} + \dots \end{aligned}$$

1. Impedance of Coated Beam Tube Alone

The measurable impedance of the coated beam tube without kicker now follows with $R_K = 0$ as

$$Z_B \sim \frac{l_K}{2\pi} \frac{j\omega R_{sq} (1 - 1/\epsilon) \ln(r_D/r_B)}{R_{sq} + j\omega r_B (1 - 1/\epsilon) \ln(r_D/r_B)}$$

which obviously represents the surface impedance of coating resistance and beam tube inductance in parallel.

2. Impedance of Kicker with High-Resistance Coated Beam Tube

Finally, the result for the measurable impedance of the kicker with high-resistance coating ($R_{sq} \sim \infty$) beam tube is found to be

$$Z_K \sim \frac{l_K}{2\pi} \frac{R_K + j\omega r_W (1 - 1/\epsilon) \ln(r_D/r_B)}{r_W + j\omega R_K \left[\epsilon(r_D^2 - r_B^2) + (r_W^2 - r_D^2) \right]}$$

which at sufficiently low frequencies becomes

$$Z_K \approx Z_{K0} + j \frac{\omega l_K}{2\pi} \left(1 - \frac{1}{\epsilon} \right) \ln \frac{r_D}{r_B}$$

representing the sum of the impedance of the kicker alone plus that of the beam tube.